J Ind Microbiol Biotechnol (2013) 40:1015–1022
DOI 10.1007/s10295-013-1297-z

ENVIRONMENTAL MICROBIOLOGY

# Use of real-time QPCR in biokinetics and modeling of two different ammonia-oxidizing bacteria growing simultaneously

**Kyungjin Cho · Duong Xuan Nguyen · Seungyong Lee · Seokhwan Hwang**

Received: 11 March 2013 / Accepted: 24 May 2013 / Published online: 6 July 2013


**Abstract** A real-time quantitative polymerase chain reaction (QPCR) was used to evaluate biokinetic coefficients of *Nitrosomonas nitrosa* and *N. cryotolerans* clusters growing simultaneously in a batch mode of ammonia oxidation. The mathematical models based on Monod equation were employed to describe the competitive relationship between these clusters and were fitted to experimental data to obtain biokinetic values. The maximum growth rates ($\mu_m$), half-saturation coefficients ($K_S$), microbial yields ($Y$) and decay coefficients ($k_d$) of *N. nitrosa* and *N. cryotolerans* were 1.77 and 1.21 $day^{-1}$, 23.25 and 23.06 mg $N{\cdot}L^{-1}$, $16 \times 10^8$ and $1 \times 10^8$ copies·mg $N^{-1}$, 0.26 and 0.20 $day^{-1}$, respectively. The estimated coefficients were applied for modeling continuous operations at various hydraulic retention times (HRTs) with an influent ammonia concentration of 300 mg $N{\cdot}L^{-1}$. Modeling results revealed that ammonia oxidation efficiencies were achieved 55–98 % at 0.8–10 days HRTs and that the system was predicted to be washed out at HRT of 0.7 days. Overall, use of QPCR for estimating biokinetic coefficients of the two AOB cluster growing simultaneously by use of ammonia were successful. This idea may open a new direction towards biokinetics of ammonia oxidation in which respirometry tests are usually employed.

Kyungjin Cho and Duong Xuan Nguyen are first authors.

K. Cho · D. X. Nguyen · S. Hwang (✉)
School of Environmental Science and Engineering,
Pohang University of Science and Technology (POSTECH),
San 31, Hyoja-dong, Nam-gu, Pohang,
Kyungbuk 790-784, Republic of Korea
e-mail: shwang@postech.ac.kr

S. Lee
R and D Center, POSCO E&C, Incheon, Republic of Korea

**Keywords** Ammonia oxidation · Model · Parameter · QPCR · 16S rRNA gene

## Introduction

Biokinetic models describe the relationship between microbial growth and substrate utilization in ecosystems. These models can help increase the understanding of the biochemical reactions and guide appropriate design, operation, and control of biology-based technologies, including biological wastewater treatment processes [19]. For this reason, numerous studies of the biokinetic of biological processes have been conducted [8, 13, 21].

Measurements of microbial concentrations are crucial for identifying and estimating parameters of biokinetic models, but accurate determination of parameters is usually problematic. They have been measured by quantifying changes (i.e., dX/dt) in volatile suspended solids (VSS), chemical oxygen demand (COD) [23], most probable number (MPN) [6], optical density, and total DNA mass [13]. However, these measures cannot distinguish microorganisms from organic materials, and cannot easily measure populations of slow-growing microorganisms such as nitrifying bacteria or methanogens accurately. The most probable number method can be used to enumerate microbial populations but this approach is time-consuming, tedious, and normally underestimates microbe numbers due to cell clumping and cell aggregation on sludge flocs [22].

Recently, quantitative real-time polymerase chain reaction (QPCR) has been proven to be a rapid and reliable tool to quantify populations of targeted microorganisms [14, 31]. Particularly, this method can effectively quantify populations of slow-growing microorganisms (i.e.,

doubling time >8 h) such as methanogens [31] and ammonia-oxidizing bacteria (AOB) [16, 22].

Applications of QPCR in biokinetic studies have been investigated in attached-growth nitrification [10] and suspended-growth nitrification [15], and in model simulation of methanogenic archaea [26]. However, the QPCR data were not used directly in parameter estimation, and several parameters (e.g., growth yield and decay coefficient) were not estimated simultaneously. Finally, application of QPCR for parameter estimation and uncertainty analysis were not fully investigated.

For slow-growing microorganisms (e.g., nitrifiers), one species has one 16S rRNA gene operon copy number per genome [7, 25]. In this case, we can use the 16S rRNA gene concentrations directly in biokinetics because they can be considered as the microbial concentrations. As a result, use of QPCR is similar to the MPN method in biokinetics [6, 28], but with several advantages (e.g., more reliable and faster analysis) as mentioned above.

The purpose of this study was to evaluate whether QPCR data can be used to directly estimate biokinetic parameters of multiple AOB species occurring simultaneously on the same substrate in an ammonia oxidizing process treating industrial wastewater in batch mode. Parameter uncertainties were also investigated to assess the quality of parameter estimates. Modeling with the estimated biokinetic parameters was also performed to predict the ammonia oxidation of the same industrial wastewater in continuous operation mode.

## Materials and methods

### Experimental setup

#### *Operation and analytical methods*

An inoculum system (IS) with 7-L working volume was used to obtain a constant source of inoculum for the biokinetic study. Sludge from an aerobic process treating industrial wastewater was collected in Pohang, Korea, and cultivated at 28 ± 2 °C and pH 7.5 with a hydraulic retention time (HRT) of 10 days. Substrate that contains a high concentration (300 mg $N{\cdot}L^{-1}$) of ammonia was obtained from the same wastewater plant.

For the biokinetic experiment, a separate completely stirred tank reactor (CSTR) with 6-L working volume was used to culture AOB in batch mode. The reactor was inoculated with 10 % (v/v) steady-state sludge from the IS. The main components of wastewater used in this study include: 281.7 mg $NH_4^+$-$N{\cdot}L^{-1}$, 6 mg $NO_2^-$-N $L^{-1}$, 6.4 mg$\cdot L^{-1}$ $NO_3^-$, and 28.7 mg $PO_4^{3-}{\cdot}L^{-1}$. The batch system was operated at 28 ± 2 °C, pH 7.5, and minimum dissolved oxygen (DO) concentration was maintained at 2 mg$\cdot L^{-1}$ to avoid inhibition of AOB growth by low DO. Concentrations of $NH_4^+$-N, $NO_2^-$-N, $NO_3^-$-N, and $PO_4^{3-}$ were measured using identical ion-exchange chromatography (Personal 790 IC, Metrohm, Switzerland).

This wastewater was collected from the steel processing factory with an advanced technology that produced much lower concentrations of ammonia and almost no toxic materials (e.g., cyanides, phenol, or heavy metals) compared to reported coke wastewaters [30]. Therefore, this wastewater can be treated directly in biological processes without pretreatment by physicochemical processes.

In the subsequent unit presentation, $NH_4^+$-N and 16S rRNA gene copies are denoted as "N" and "copies", respectively; thus substrate concentration and half-saturation coefficient have units of mg $N{\cdot}L^{-1}$ growth yield has units of copies$\cdot$mg $N^{-1}$.

#### *DNA extraction*

Mixed liquor suspended solid (MLSS) samples were collected, centrifuged at 14,000 rpm for 5 min, washed twice with deionized distilled water, and then loaded into a fully automated nucleic acid extractor (Magtration System 6GC, PSS Co., Japan) with an appropriate Genomic DNA Purification Kit (PSS) to extract total genomic DNA. Duplicated genomic DNA extracted from processed MLSS samples were immediately stored at −20 °C until they were used in QPCR.

#### *QPCR analysis*

QPCR to determine the quantities of AOB subgroups was performed using a LightCycler 1.2 (Roche Diagnostics, Mannheim, Germany). Five group-specific primer and probe sets targeting 16S rRNA genes of AOBs were previously developed for sensitive detection and quantification, where specificities of the sets were verified both in silico and in vitro (Table 1), and were used in this study.

A real-time PCR mixture of 20 μL was prepared; it consisted of 2 μL of template DNA, 1 μL each of forward primer and of reverse primer (final concentration 500 nM), 1 μL of TaqMan probe (final concentration 100 nM), 5 μL of LightCycler TaqMan Master mix (Roche Diagnostics), and 10 μL of PCR-grade water. All measurements for biokinetics including $NH_4^+$-N and 16S rRNA genes were duplicated.

Among five AOB subgroups, three species (i.e., *Nitrosomonas europaea*, *N. nitrosa* and *N. cryotolerans*) were only detected in which *N. nitrosa* and *N. cryotolerans* were found to be predominant (98.6–99.9 % 16S rRNA genes of the AOB community). Correspondingly, *N. europaea* accounted for a maximum of 1.4 % 16S rRNA genes of the

**Table 1** Primers and probe sets for ammonia oxidation bacteria [14]

| Name | Target group | Sequence (5′→3′) | *E. coli* numbering |
|---|---|---|---|
| NSMeur-828F | *Nitrosomonas europaea* cluster | GTTGT CGGAT CTAAT TAAG | 828–846 |
| NSMeur-984T | | CCTAC CCTTG ACATG CTTGG AATC | 984–1007 |
| NSMeur-1028R | | TGTCT TGGCT CCCTT TC | 1028–1044 |
| NSMmob-988F | *Nitrosococcus mobilis* cluster | GCTTG GAATT TTACG GAGAC | 988–1017 |
| NSMmob-1243T | | AGTGT ACAGA GGGTA GCCAA CCC | 1243–1265 |
| NSMmob-1282R | | CTACG AAGTG CTTTG TGAG | 1282–1300 |
| NSMnit-438F | *Nitrosomonas nitrosa* cluster | TTCGG TCGGG AAGAW ATAG | 438–456 |
| NSMnit-483T | | CGGTA CCGAC ATAAG AAGCA CCGG | 483–506 |
| NSMnit-633R | | CTAGT YATAT AGTTT CAAAC GC | 633–654 |
| NSMcry-211F | *Nitrosomonas cryotolerans-cluster* | AGACC TTRTG CTTTT GGAG | 211–229 |
| NSMcry-270T | | CCAAC TACTG ATCGT YGCCT TGGT | 270–293 |
| NSMcry-434R | | TTTTC TTCTC RACTG AAAGA G | 434–454 |
| NSS-209F | *Nitrosospira* genus | CAAGA CCTTG CGCTY TT | 209–225 |
| NSS-432T | | TTTCG TTCCG GCTGA AAGAG CT | 432–453 |
| NSS-478R | | TCTTC CGGTA CCGTC AKT | 478–495 |

*F* forward primer, *T* TaqMan probe, *R* reverse primer

total AOB abundance. Therefore, we applied the models to estimate the biokinetic parameters for these two predominant AOB clusters.

## Mathematical description

The Monod equation (Eq. 1) was used in this study:

$$\mu = \frac{\mu_{\mathrm{m}} S}{K_{\mathrm{S}} + S} \tag{1}$$

where $\mu$ is the specific growth rate ($\mathrm{day}^{-1}$), $\mu_{\mathrm{m}}$ is the maximum specific growth rate ($\mathrm{day}^{-1}$), $K_{\mathrm{S}}$ is the half-saturation coefficient (mg $\mathrm{N{\cdot}L^{-1}}$), and $S$ is the substrate concentration (mg $\mathrm{N{\cdot}L^{-1}}$).

The "two-clusters with single substrate" system was applied to the batch system [27]:

$$\frac{dS}{dt} = -\sum_{k=1}^{2} \frac{\mu_{\mathrm{m}k}}{Y_k} \frac{S}{K_{\mathrm{S}k} + S} X_k, \quad k = 1, 2 \tag{2}$$

$$\frac{dX_k}{dt} = \left( \frac{\mu_{\mathrm{m}k} S}{K_{\mathrm{S}k} + S} - k_{\mathrm{d}k} \right) X_k \tag{3}$$

where $Y$ is growth yield (copies·mg $\mathrm{N}^{-1}$), $X$ is the microbial concentration (copies·$\mathrm{mL}^{-1}$), $k_{\mathrm{d}}$ is the microbial decay coefficient ($\mathrm{day}^{-1}$), and $k$ in subscripts represent the first (*N. nitrosa*) and second (*N. cryotolerans*) clusters.

The optimal choice of parameters was achieved by minimizing the least-squares objection function (Eq. 4) [3]:

$$J(\theta) = -\sum_{j=1}^{N_{\mathrm{var}}} W_j \sum_{i=1}^{N_{\mathrm{data}}} \left[ \left( y(t_{ji}, \theta) - y(t_{ji}) \right) \right]^T W_{ji} \left[ \left( y(t_{ji}, \theta) - y(t_{ji}) \right) \right] \tag{4}$$

where $N_{\mathrm{var}}$ is the number of output variables (i.e., $S$, $X_1$, $X_2$), $N_{\mathrm{data}}$ is the number of data points, $\theta(\mu_{\mathrm{m1}}, K_{\mathrm{S1}}, Y_1, k_{\mathrm{d1}}, \mu_{\mathrm{m2}}, K_{\mathrm{S2}}, Y_2, k_{\mathrm{d2}})$ is the parameter vector, $y(t_{ji})$ is the measurement data, and, $y(t_{ji}, \theta)$ is the model predictions. Eq. (4) includes two weighted functions: the first ($W_j$) is a vector that weights the differences among three output variables; the second ($W_{ji}$) is a square matrix with user-supplied weighting coefficients that weights the differences among measured values within each output (e.g., $S_1,\ldots,S_{\mathrm{Ndata}}$). Commonly, $W_j$ is chosen such that $\sum_{j=1}^{N_{\mathrm{var}}} W_j = 1$ and $W_j > 0$ [17]; thus the values of $W_j$ were changed for each minimization search.

Confidence intervals of all parameters and correlations among parameters within each parameter sets were determined from the covariance matrix (V), which is the inverse of the Fisher information matrix (FIM) [3].

$$\mathrm{FIM}_j = \sum_{i=1}^{N_{\mathrm{data}}} \left( \frac{\partial y}{\partial \theta}(t_{ji}, \theta_k) \right)^T W_{ji} \left( \frac{\partial y}{\partial \theta}(t_{ji}, \theta_k) \right), \quad j = 1, 2, 3, 4; \quad k = 1, 2 \tag{5}$$

$$V_j = \mathrm{FIM}_j^{-1} \tag{6}$$

where $\partial y / \partial \theta$ are the sensitivity functions and $W_{ji}$ is the weighting function, which is also the square weighting matrix in Eq. (4). Because there were four different sensitivity functions (i.e., $\partial S/\partial\theta_1$, $\partial X_1/\partial\theta_1$, $\partial S/\partial\theta_2$, $\partial X_2/\partial\theta_2$), four FIM matrices and four covariance matrices were computed. As a result, there were two covariance matrices for one parameter set ($\theta_1 = [\mu_{m1}, K_{S1}, Y_1, k_{d1}]$ or$\theta_2 = [\mu_{m2}, K_{S2}, Y_2, k_{d2}]$). Thus which covariance matrix

gives the larger confidence intervals or parameter errors will be selected.

## Results

### Performance of ammonia-oxidation system

During the first step of the nitrification process, concentrations of ammonia and *Nitrosomonas* clusters began to change after a lag period of about 3 days of incubation (Fig. 1). The initial concentration of ammonia, 281.7 mg·L$^{-1}$, was oxidized completely after 6.8 days of incubation. The initial 16S rRNA gene copy numbers for the *N. nitrosa* and *N. cryotolerans* were $2.2 \times 10^5$ and $3.5 \times 10^5$ copies·mL$^{-1}$, respectively. After the lag period, the 16S rRNA gene concentrations of *N. nitrosa* and *N. cryotolerans* increased rapidly and reached maxima of $2.1 \times 10^7$ and $2.2 \times 10^7$ copies·mL$^{-1}$ at 7.3 and 9.8 days, respectively. Measured abundance of 16S rRNA genes indicated that *N. nitrosa* and *N. cryotolerans* comprised 98.6–99.9 % of the AOB community in the reactor.

### Parameter estimation and uncertainty analysis

The models were fitted to the experimental data of ammonia, *N. nitrosa*, and *N. cryotolerans* to evaluate biokinetic parameters (Fig. 1). The models all had acceptable fits ($r^2 > 0.9$).

Parameter estimates for two AOB clusters are presented in Table 2. The maximum specific growth rate of *N. nitrosa* (1.77 day$^{-1}$) was higher than that of *N. cryotolerans* (1.21 day$^{-1}$), probably because right after the lag phase the former showed a sharper increase in growth rate than did the latter. In contrast, at day 3 (beginning of biokinetic analysis) the 16S rRNA gene concentration of *N. cryotolerans* was twice that of *N. nitrosa*. The growth yield of *N. nitrosa* ($16 \times 10^8$ copies·mg N$^{-1}$) was also higher than that of *N. cryotolerans* ($1 \times 10^8$ copies·mg N$^{-1}$), indicating that the former harvested more of the available energy for cell growth than did the latter. The decay coefficient ($k_d$) of *N. nitrosa* was 1.3 times that of *N. cryotolerans*. In contrast, the half-saturation coefficients ($K_S$) of the two *Nitrosomonas* clusters were identical (23 mg N·L$^{-1}$), implying that they have a similar affinity for the substrate.

Although eight parameters were estimated, only five parameters ($\mu_{m1}$, $k_{d1}$, $\mu_{m2}$, $Y_2$, $k_{d2}$) were identifiable with the 95 % confidence interval (CI) (Table 2). In addition, because the CI of $Y$ for *N. nitrosa* ($38.3 \times 10^8$ copies·mg N$^{-1}$) was higher than the parameter value ($16.0 \times 10^8$ copies·mg N$^{-1}$), this $Y$ estimate was also not identifiable.

Along with the parameter estimation and confidence intervals, correlation coefficients of the two *Nitrosomonas*

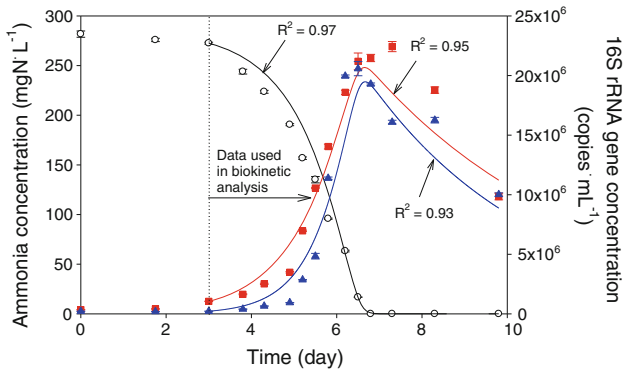


**Fig. 1** Changes in concentrations of $NH_4^+$-N (*open circles*, *left* y-axis), *N. nitrosa* (*blue*, *right* y-axis) and *N. cryotolerans* (*red*, *right* y-axis). *Points* measurement; *lines* model predictions. *Bars* ± standard deviation when larger than the symbols

**Table 2** Estimated biokinetic coefficients and 95 % confidence intervals

| Parameters | Values | |
|---|---|---|
| | *N. nitrosa* | *N. cryotolerans* |
| $\mu_m$ (day$^{-1}$) | 1.77 ± 0.98 (<0.01) | 1.21 ± 0.06 (<0.01) |
| $K_S$ (mg N·L$^{-1}$) | 23.25 | 23.06 |
| $Y$ ($10^8$ copies·mg N$^{-1}$) | 16.00 ± 38.27 (3.18) | 1.00 ± 0.06 (0.01) |
| $k_d$ (day$^{-1}$) | 0.26 ± 0.14 (0.01) | 0.20 ± 0.07 (<0.01) |

CIs from covariance matrices based on microbial outputs are in *parentheses*

**Table 3** Correlation matrix of biokinetic parameters for *N. nitrosa*

| | $\mu_m$ | $Y$ | $k_d$ |
|---|---|---|---|
| $\mu_m$ | 1.00 | | |
| $Y$ | 0.98 (0.59) | 1.00 | |
| $k_d$ | 0.86 (0.92) | 0.84 (0.86) | 1.00 |

Correlation coefficients from covariance matrix based on microbial outputs are in *parentheses*

**Table 4** Correlation matrix of biokinetic parameters for *N. cryotolerans*

| | $\mu_m$ | $Y$ | $k_d$ |
|---|---|---|---|
| $\mu_m$ | 1.00 | | |
| $Y$ | 0.51 (0.76) | 1.00 | |
| $k_d$ | 0.93 (0.89) | 0.15 (0.94) | 1.00 |

Correlation coefficients from covariance matrix based on microbial outputs are in *parentheses*

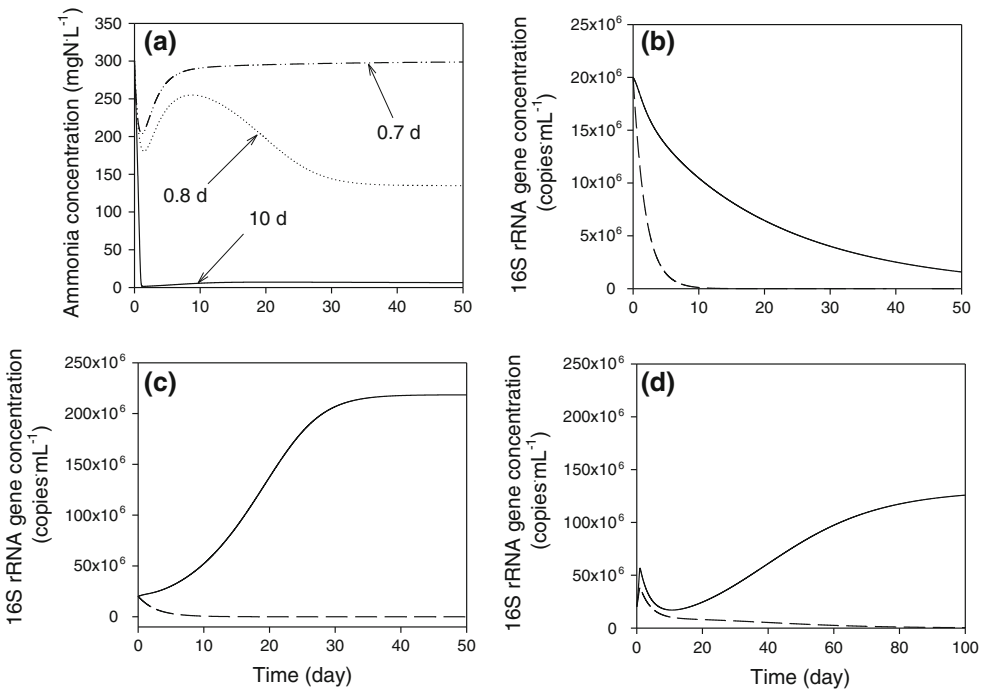


**Fig. 2** **a** Predicted residual concentrations of $NH_4^+$-N at different HRTs during continuous-mode ammonia oxidation of industrial wastewater. Corresponding concentrations of *N. nitrosa* (*solid line*) and *N. cryotolerans* (*broken line*) predicted at HRTs of **b** 0.7 days, **c** 0.8 days, and **d** 10 days

clusters were derived from the covariance matrix (Tables 3, 4). Correlations between most parameter pairs were <0.9, which is considered to be the threshold of high correlation [24]. However, for *N. nitrosa* one pair had correlation >0.9: $\mu_m$ versus $Y$ (0.98); and for *N. cryotolerans* one pair had correlation >0.9: $\mu_m$ versus $k_d$ (0.93).

### Application of estimated parameters to a continuous ammonia oxidation system

Using the parameters estimated in batch mode, changes in the concentrations of *N. nitrosa*, *N. cryotolerans*, and residual ammonia were predicted if the batch system would start at different flow rates (i.e., different hydraulic retention times) with the two species of AOBs. In continuous mode, HRT ($\tau$) was incorporated into the rate equations (Eqs. 2 and 3) as follows

$$\frac{dS}{dt} = \frac{S_{\text{inf}} - S}{\tau} - \sum_{k=1}^{2} \frac{\mu_{\text{mk}}}{Y_k} \frac{S}{K_{\text{Sk}} + S} X_k, \quad k = 1, 2 \tag{7}$$

$$\frac{dX_k}{dt} = \left( \frac{\mu_{\text{mk}} S}{K_{\text{Sk}} + S} - k_{\text{dk}} - \frac{1}{\tau} \right) X_k \tag{8}$$

where $S_{\text{inf}}$ (mg N·L$^{-1}$) is the influent substrate concentration. The initial concentrations of ammonia and *N. nitrosa* and *N. cryotolerans* 16S rRNA genes in the bioreactor were 300 mg·L$^{-1}$ and $2 \times 10^7$ copies·mL$^{-1}$, respectively. The influent nitrogen concentration was assumed to be 300 mg·L$^{-1}$; the influent concentrations of *N. nitrosa* and *N. cryotolerans* were assumed to be zero. These concentrations were selected based on the batch experiment.

The changes in concentrations of $NH_4^+$-N and 16S rRNA genes of *N. nitrosa* and *N. cryotolerans* clusters were simulated at different HRT (Fig. 2). The residual $NH_4^+$-N concentrations decreased and remained at steady state at HRT >0.7 days. This HRT was considered as the washout point at which the $NH_4^+$-N concentration remained similar to the influent level after 10 days of incubation (Fig. 2a) and the microorganisms were washed out (Fig. 2b). At steady state (i.e., 0.8 days ≤ HRT ≤ 10 days), the expected $NH_4^+$-N oxidation efficiencies ranged from 55 to 98 % (Fig. 2a), corresponding to the increase of *N. nitrosa* 16S rRNA gene concentrations (Fig. 2c, d). *N. nitrosa* completely outcompeted *N. cryotolerans* when the reactor approached the steady state.

## Discussion

The idea of biokinetics based on two or more species (or groups) in wastewater treatment is based on the number of predominant species (or groups). In the rate equations presented here, the concentrations of the substrate and of predominant species (or groups) are denoted as state variables ($S$, $X_1$, and $X_2$). Among five subgroups of AOB (i.e., genus *Nitrosospira* and four *Nitrosomonas* clusters) commonly used in wastewater systems [14, 15], three *Nitrosomonas* clusters (i.e., *N. europaea* (data not shown), *N. nitrosa,* and *N. cryotolerans*) were detected and two (i.e.,

*N. nitrosa* and *N. cryotolerans*) were predominant. The *N. europaea* cluster, which is the most frequently isolated and investigated because it usually outcompetes other AOB in $NH_4^+$-N-rich environments [15], was found to have little influence in this study. This result contradicts a previous finding in our laboratory in which the *N. europaea* cluster outcompeted the *N. nitrosa* cluster [15]. This discrepancy may be due to differences in substrate and seeding sludge (i.e., different industrial wastewaters) used in the ISs and in the biokinetic batch reactors. Based on microbial data in this study, two *Nitrosomonas* clusters along with substrate were selected for the biokinetic analysis.

In biokinetic analysis, one important task is to practically identify the estimated parameters to evaluate the reliability of parameter values. As seen in the uncertainty analysis (Table 2), five parameter estimates ($\mu_{m1}$, $k_{d1}$, $\mu_{m2}$, $Y_2$, $k_{d2}$) were identifiable practically, but three others ($K_{S1}$, $Y_1$, $K_{S2}$) were not. Attempts to identify all parameters were not successful because FIMs were singular and could not be inverted to obtain corresponding covariance matrices. The singularity of FIMs was due to the linearly dependence between the sensitivity functions of $\mu_m$ and $K_S$ (data not shown). Hence, one of these dependent functions should be excluded to avoid the singularity [21]. In this study, the sensitivity functions of $K_S$ were removed from the FIMs, so the CIs of $K_S$ for both *N. nitrosa* and *N. cryotolerans* were not estimated. Finally, $Y_1$ was not identifiable practically, possibly due to the limited number (i.e., 13) of data points [24].

In addition to estimation of parameter uncertainties, determination of the correlation of parameter pairs is also important in practical identifiability. If the correlation coefficient between two parameters is zero or close to zero, they are linearly independent, and this is the most desirable condition in biokinetic analysis. However, if it is >0.9, the pair is considered highly correlated [24]; compared to the zero-correlation case this condition is less desirable because a change in one parameter will be counteracted by a corresponding change of the correlated parameter while still maintaining good model predictions; this results in a broad range of parameter estimates [9, 21]. One parameter pair of *N. nitrosa* and one pair of *N. cryotolerans* were highly correlated (i.e., >0.9) in this study (Tables 3, 4) probably because the models were based on the Monod equation, which is well known for high correlation among parameters [9, 18, 29]. Nevertheless, all of the correlation coefficients were <0.99 (the threshold to cause the FIM to be singular [11], so the FIM excluding $K_S$ could be successfully inverted. Obviously, optimal experimental design should be used to reduce or even eliminate the linear dependence among parameters [2, 3], but this topic is beyond the scope of this work.

The parameter uncertainties for estimated parameters were determined both based on substrate and microbial outputs because each parameter sets ($\theta_1$, $\theta_2$) has two covariance matrices as explained in Eqs. (5) and (6). CIs estimated from covariance matrices based on substrate outputs are clearly larger than those from microbial ones (Table 2). As a result, the former CIs were selected to ensure that the parameter estimates fall within the intervals with 95 % probability. However, not all the correlations from covariance matrices based on microbial outputs were smaller than those based on substrate (Tables 3, 4). Thus, the correlations based on substrate are still chosen to maintain consistency with the CI results.

Because no similar reports for dual-cluster biokinetic with similar *Nitrosomonas* clusters exist, the present results cannot be compared directly with others. In a previous study [15], calculated $\mu_m$ for *N. nitrosa* clusters was 0.36 $day^{-1}$ for, but this value was simply approximated during exponential growth, and did not include uncertainty analysis. In this study, the *N. nitrosa* cluster had $\mu_m = 1.77$ $day^{-1}$, five times larger than the previously report [15]. The difference between these $\mu_m$ estimates for the *N. nitrosa* cluster indicate that experiment conditions for biokinetic analysis for system design and control should be established carefully. These conditions (e.g., substrate, inoculum source, operational conditions) in the applied system should be as identical as possible to those in the biokinetic experiment system.

The biokinetic results with high-strength ammonia oxidation (500–1,000 mg $N{\cdot}L^{-1}$) in a sequencing bioreactor based on respirometric method [20] might be used as a reference. The values of $\mu_m$ and $k_d$ of aggregated AOB were 1.96 $day^{-1}$ and 0.44 $day^{-1}$, respectively [20], which are similar to our estimates of $\mu_m$ (1.77 and 1.21 $day^{-1}$) and $k_d$ (0.26 and 0.20 $day^{-1}$). These results suggest that the $\mu_m$ and $k_d$ when high-strength $NH_4^+$-N wastewater is used are much higher than those (i.e., $\sim$1.0 and 0.15 $day^{-1}$ at 25 °C, [23]) when low-strength $NH_4^+$-N wastewater is used (e.g., <50 mg $N{\cdot}L^{-1}$ for domestic wastewater).

The $K_S$ values (23 mg $N{\cdot}L^{-1}$) in this study were much higher than those for industrial wastewater (0.5 mg $N{\cdot}L^{-1}$) [20] and those for domestic wastewater (0.5–1.0 mg $N{\cdot}L^{-1}$) [23]. This difference indicates that both *N. nitrosa* and *N. cryotolerans* had low affinity to the ammonia in industrial wastewater used in this study. The high $K_S$ value might be an effect of high substrate concentration [5], high correlation with $\mu_m$, or both.

Both *N. nitrosa* and *N. cryotolerans* were predicted to wash out at HRT = 0.7 days, resulting in a rapid increase in the residual ammonia concentration to the initial concentration of 300 mg $N{\cdot}L^{-1}$. The unstable behavior of the system at 0.8 days HRT implies that a very small change in flow rate near the washout point could have a large effect

on the system performance [1]. Thus, the reciprocal of 0.8 days HRT (i.e., 1.25 $day^{-1}$), which is higher than the $\mu_m$ of *N. cryotolerans* but lower than that of *N. nitrosa*, is considered as the threshold to distinguish the behaviors of the two *Nitrosomonas* clusters right after simulation (Fig. 2c). When HRT was 10 days, the ammonia concentrations reached steady state after 2 days of operation while the microbial community was still at dynamic conditions; this result agrees with previous reports of dynamic microbial states [4, 12]. The outcompeting *N. nitrosa* is predicted to be dominant over *N. cryotolerans* in the system, particularly under steady-state conditions. However, considering the variations in flow-rate, substrate characteristics, nutrients, and environmental conditions, several *Nitrosomonas* clusters can coexist.

This paper demonstrated successful application of QPCR in biokinetic analysis of the ammonia oxidation process by two *Nitrosomonas* clusters. Among eight parameters, five were identifiable. Modeling showed that the dynamic populations could maintain good ammonia oxidation efficiency. Modeling with an ideal CSTR system could not demonstrate the diversity of the microbial community usually seen in real wastewater systems because the variations in flowrate, influent concentration, nutrients, and environmental factors were not considered. However, the application of QPCR for analysis of biokinetics shows good promise for ammonia oxidation in which respirometry tests are usually employed.

**Acknowledgments** This work was supported by the New and Renewable Energy Technology R and D program of the Korea Institute of Energy Technology Evaluation and Planning (KETEP) grant funded by the Korean Ministry of Knowledge Economy (Grant No. 20103020090050).

## References

1. Ahn J-H, Kim J, Lim J, Hwang S (2004) Biokinetic evaluation and modeling of continuous thiocyanate biodegradation by *Klebsiella* sp. Biotechnol Progr 20(4):1069–1075
2. Chandran K, Smets BF (2005) Optimizing experimental design to estimate ammonia and nitrite oxidation biokinetic parameters from batch respirograms. Water Res 39(20):4969–4978
3. Dochain D, Vanrolleghem P (2001) Dynamical modelling and estimation in wastewater treatment processes. IWA Publishing, Colchester
4. Fernández A, Huang S, Seston S, Xing J, Hickey R, Criddle C, Tiedje J (1999) How stable is stable? Function versus community composition. Appl Environ Microbiol 65(8):3697–3704
5. Grady CPL Jr, Smets BF, Barbeau DS (1996) Variability in kinetic parameter estimates: a review of possible causes and a proposed terminology. Water Res 30(3):742–748
6. Hall ER, Murphy KL (1980) Estimation of nitrifying biomass and kinetics in wastewater. Water Res 14(4):297–304
7. Harms G, Layton AC, Dionisi HM, Gregory IR, Garrett VM, Hawkins SA, Robinson KG, Sayler GS (2002) Real-time PCR quantification of nitrifying bacteria in a municipal wastewater treatment plant. Environ Sci Technol 37(2):343–351
8. Henze M, Gujer W, Mino W, van Loosdrecht MCM (2000) Activated sludge models ASM1, ASM2, ASM2d and ASM3. IWA Publishing, London
9. Holmberg A (1982) On the practical identifiability of microbial growth models incorporating Michaelis–Menten-type nonlinearities. Math Biosci 62(1):23–43
10. Kindaichi T, Kawano Y, Ito T, Satoh H, Okabe S (2006) Population dynamics and in situ kinetics of nitrifying bacteria in autotrophic nitrifying biofilms as determined by real-time quantitative PCR. Biotechnol Bioeng 94(6):1111–1121
11. Landaw EM, DiStefano JJ (1984) Multiexponential, multicompartmental, and noncompartmental modeling. II. Data analysis and statistical considerations. Am J of Physiol Regul Integr Comp Physiol 246(5):R665–R677
12. Layton AC, Dionisi H, Kuo H-W, Robinson KG, Garrett VM, Meyers A, Sayler GS (2005) Emergence of competitive dominant ammonia-oxidizing bacterial populations in a full-scale industrial wastewater treatment plant. Appl Environ Microbiol 71(2): 1105–1108
13. Lee C, Kim J, Hwang K, Hwang S (2009) Fermentation and growth kinetic study of *Aeromonas caviae* under anaerobic conditions. Appl Microbiol Biotechnol 83(4):767–773
14. Lim J, Do H, Shin SG, Hwang S (2008) Primer and probe sets for group-specific quantification of the genera *Nitrosomonas* and *Nitrosospira* using real-time PCR. Biotechnol Bioeng 99(6): 1374–1383
15. Lim J, Lee S, Hwang S (2008) Use of quantitative real-time PCR to monitor population dynamics of ammonia-oxidizing bacteria in batch process. J Ind Micropbiol Biotechnol 35(11):1339–1344
16. Lipponen MTT, Suutari MH, Martikainen PJ (2002) Occurrence of nitrifying bacteria and nitrification in Finnish drinking water distribution systems. Water Res 36(17):4319–4329
17. Marler RT, Arora JS (2004) Survey of multi-objective optimization methods for engineering. Struct Multidiscip O 26(6):369–395
18. Marsili-Libelli S (1992) Parameter estimation of ecological models. Ecol Model 62(4):233–258
19. Olsson G, Newell B (1999) Wastewater treatment systems: modelling, diagnosis and control. IWA Publishing, London
20. Pambrun V, Paul E, Spérandio M (2006) Modeling the partial nitrification in sequencing batch reactor for biomass adapted to high ammonia concentrations. Biotechnol Bioeng 95(1):120–131
21. Petersen B, Gernaey K, Vanrolleghem PA (2001) Practical identifiability of model parameters by combined respirometric-titrimetric measurements. Wat Sci Tech 43(7):347–355
22. Purkhold U, Pommerening-Röser A, Juretschko S, Schmid MC, Koops H-P, Wagner M (2000) Phylogeny of all recognized species of ammonia oxidizers based on comparative 16S rRNA and amoA sequence analysis: implications for molecular diversity surveys. Appl Environ Microbiol 66(12):5368–5382
23. Rittmann BE, McCarty PL (2001) Environmental biotechnology: principles and applications. McGraw-Hill Inc., New York
24. Robinson JA (1985) Determining microbial kinetic parameters using nonlinear regression analysis. In: Marshall KC (ed) Advances in microbial ecology. Plenum Press, New York, pp 61–114
25. Robinson KG, DiStefano JJ, Harms G, Layton AC, Gregory IR, Sayler GS (2003) Molecular assessment of ammonia- and nitrite-oxidizing bacteria in full-scale activated sludge wastewater treatment plants. Wat Sci Tech 48(8):119–126
26. Shin S, Lee C, Hwang K, Ahn J-H, Hwang S (2008) Use of order-specific primers to investigate the methanogenic diversity in acetate enrichment system. J Ind Microbiol Biotechnol 35(11): 1345–1352

27. Shuler ML, Kargi F (2002) Bioprocess engineering: basic concepts. Prentice-Hall Inc., New Jersey
28. Utgikar VP, Tabak HH, Haines JR, Govind R (2003) Quantification of toxic and inhibitory impact of copper and zinc on mixed cultures of sulfate-reducing bacteria. Biotechnol Bioeng 82(3):306–312
29. Vanrolleghem P, Keesman KJ (1996) Identification of biodegradation models under model and data uncertainty. Wat Sci Tech 33(2):91–105
30. Vázquez I, Rodríguez J, Marañón E, Castrillón L, Fernández Y (2006) Simultaneous removal of phenol, ammonium and thiocyanate from coke wastewater by aerobic biodegradation. J Hazard Mater 137(3):1773–1780
31. Yu Y, Lee C, Kim J, Hwang S (2005) Group-specific primer and probe sets to detect methanogenic communities using quantitative real-time polymerase chain reaction. Biotechnol Bioeng 89(6):670–679